

Statistical correlation for the composite Boson

Baigeng Wang and Jian Wang^{a)}

Department of Physics, The University of Hong Kong, Pokfulam Road, Hong Kong, China

It is well known that the particles in a beam of Boson obeying Bose-Einstein statistics tend to cluster (bunching effect), while the particles in a degenerate beam of Fermion obeying Fermi-Dirac statistics expel each other (anti-bunching effect). Here we investigate, for the first time, the statistical correlation effect for the composite Boson, which is formed from a spin singlet entangled electron pair. By using nonequilibrium Green's function technique, we obtain a positive cross correlation for this kind of the composite Boson when the external voltage is smaller than the gap energy, which demonstrates that a spin singlet entangled electron pair looks like a composite Boson. In the larger voltage limit, the cross correlation becomes negative due to the contribution of the quasiparticles. At large voltages, the oscillation between Fermionic and Bosonic behavior of cross correlation is also observed in the strong coupling regime as one changes the position of the resonant levels. Our result can be easily tested in a three-terminal normal-superconductor-superconductor (N-S-S) hybrid mesoscopic system.

74.50.+r, 72.70.+m, 74.40.+k, 73.23.-b

I. INTRODUCTION

There are two kinds of quantum statistics in nature. All particles have either half-integral or integral spin (in units of the Plank constant \hbar) and they obey Fermi-Dirac¹ or Boson-Einstein² statistics respectively. It is also noted³ that there is an effective attraction between the Bosons and an effective repulsion between the Fermions. This is the well known statistical correlation effects⁴, which are purely quantum effect. The experiments examining the quantum statistical properties date back to the pioneer work, by Hanbury Brown and Twiss (HBT)⁵. They used photon intensity interferometry to probe the intensity correlation information between two partial beams, which was generated by a beam splitter. Due to the Bosonic property of photon, the positive intensity correlation was observed, indicating an enhanced probability for the simultaneous detection of two photons, one in each partial beam. This means that photons tend to bunch in cluster. Several theoretical works have suggested the different analogies of this experiment with electrons in mesoscopic systems. The Fermionic analog of HBT experiments, one by Henny et al.⁶ and the other by Oliver et al.⁷, showed the expected negative intensity correlation and observed the anti-bunching effect. In this paper we will investigate the HBT experiment for the composite Boson. This composite Boson is formed by a spin singlet entangled electron pair, which will be

discussed below. Due to the zero total spin for the entangled electron pair, we expect that these composite Bosons tend to bunch in cluster. Motivated by the application in quantum communication and computation, Burkard et al⁸ have studied entangled electrons in an interacting many-body environment. They found that the Fano factor for singlets is twice as large as for independent classical particles and is reduced to zero for triplets. Torriès and Martin⁹ investigated a three-terminal N-N-S mesoscopic system, both positive and negative correlations were found in the Andreev regime. Very recently, Samueisson and Büttiker¹⁰ studied the same structure and found the positive correlation for a wide range of junction parameters which survives even in the absence of the proximity effect. The statistics of charge transport of a three terminal N-N-S beam splitter has also been investigated¹¹ and positive cross correlation is found between the currents in two normal leads for a wide parameter range. Instead of the structures of the references 9–11, here we consider a three-terminal mesoscopic N-S-S hybrid system. This structure is a direct photon analogy of the HBT interferometer which has a normal lead and two superconducting leads. A quantum dot, connected by these three terminals, acts as a splitter. Suppose that the chemical potentials μ_s for both superconducting reservoirs are set to zero, and the chemical potential for the normal is above zero, i.e., $eV > 0$, which guarantees the electron current passing from the normal lead to both superconducting leads. We further assume the temperature is very low. If the external voltage eV is smaller than the gap energy Δ of the superconducting leads, the single quasiparticle current is forbidden. In this case, we only have two-electron current due to the presence of Andreev reflection process, i.e., incoming electrons being Andreev reflected into outgoing holes with the transfer of a Cooper pair into the superconductor. This means that an electron (with energy ϵ above the Fermi level and spin σ) in the normal lead, has to combine another electron (with energy $-\epsilon$, below the Fermi level and spin $-\sigma$) to pass through the NS interface. Does this entangled electron pair¹² look like a composite Boson? or rather, can we obtain a positive cross correlation function ($\langle \Delta I_\alpha \Delta I_\beta \rangle$ with $\alpha \neq \beta$) between two superconducting leads? The purpose of this paper is to answer this question. We note that due to the current conservation the cross correlation function of a two-lead system must be negative regardless of normal or superconducting leads. Instead of considering the fluctuation in a single electron beam through the two-lead system, the HBT experiment considered here focuses on the cross correlation of two beams from the beam splitter. Hence we expect positive

cross correlation at small voltages which is indeed what we found in this work. When $eV > \Delta$, the quasiparticles will also participate the transport. Due to the Fermionic nature of quasiparticles, it will partially cancel the positive contribution of the entangled electron pair to the cross correlation. The competition of these two contributions from the entangled electron pair and quasiparticles can lead to either positive or negative cross correlation depending on which contribution dominates.

II. THEORETICAL FORMULATION

We begin with the following model Hamiltonian

$$H = \sum_p \epsilon_p C_{1,p\sigma}^+ C_{1,p\sigma} + \sum_{kn} [\sum_{\sigma} \epsilon_k C_{n,k\sigma}^+ C_{n,k\sigma} + \Delta C_{n,k\uparrow}^+ C_{n,-k\downarrow}^+ + \Delta C_{n,-k\downarrow} C_{n,k\uparrow}] + \sum_{\sigma} \epsilon_0 d_{\sigma}^{\dagger} d_{\sigma} + \sum_{p\sigma} [T_{1,p} C_{1,p\sigma}^+ d_{\sigma} + c.c.] + \sum_{kn\sigma} [T_{n,k} C_{n,k\sigma}^+ d_{\sigma} + c.c.] \quad (1)$$

where the first term denotes the Hamiltonian of the normal lead. The second term ($n = 2, 3$) describes the Hamiltonian of two BCS superconducting leads. Here $C_{1,k\sigma}^{\dagger}$ is the creation operator of electrons in the normal lead and $C_{n,k\sigma}^{\dagger}$ is the corresponding creation operator in the superconducting lead. The third term is the Hamiltonian for a quantum dot, which is used to mimic a tunable beam splitter. Here we have applied a gate voltage which can control the level of the dot so that $\epsilon_0 = \epsilon_0^{(0)} + ev_g$. Without loss of generality, we set $\epsilon_0^{(0)} = 0$. The other terms in Eq.(1) are Hamiltonians describing the couplings between the quantum dot and leads. To simplify the discussion, we have assumed that two superconducting leads have the same gap energy Δ . We have also neglected the supercurrent between two superconducting leads¹³ and assumed that the hopping matrix elements are independent of the spin index.

In the following, we will calculate the cross correlation between two partial beams through two superconducting leads. The current operator for the superconducting lead 2 or 3 is

$$\hat{I}_{\alpha} = \hat{I}_{\alpha\uparrow}(t) + \hat{I}_{\alpha\downarrow}(t)$$

with

$$\hat{I}_{\alpha\sigma}(t) = ie [\sum_k C_{\alpha,k\sigma}^{\dagger} C_{\alpha,k\sigma}, H] = ie \sum_k [T_{\alpha k} C_{\alpha,k\sigma}^+ d_{\sigma} - c.c.]$$

where $\alpha = 2, 3$. Due to the electron-hole symmetry of the system, we have $\hat{I}_{\alpha\uparrow}(t) = \hat{I}_{\alpha\downarrow}(t)$. Hence the current operator can be rewritten as

$$\hat{I}_{\alpha}(t) = 2ie \sum_k [T_{\alpha k} C_{\alpha,k\uparrow}^+ d_{\uparrow} - c.c.]$$

The cross correlation between two superconducting leads is defined as

$$P_{23} \equiv \langle \Delta I_2(t_1) \Delta I_3(t_2) \rangle \equiv \langle [\hat{I}_2(t_1) - \bar{I}_2][\hat{I}_3(t_2) - \bar{I}_3] \rangle$$

with $\bar{I}_{\alpha} \equiv \langle \hat{I}_{\alpha} \rangle$. Here $\langle \dots \rangle$ denotes both the statistical average and quantum average on the nonequilibrium state. Using the expression of the current operator, the cross correlation between two superconducting leads is

$$P_{23} = -4e^2 \sum_{k,k'} [T_{2,k} T_{3,k'} G_{d\uparrow k\uparrow}^{<}(2,1) G_{d\uparrow k'\uparrow}^{>}(1,2) + T_{2,k}^* T_{3,k'}^* G_{k'\uparrow d\uparrow}^{<}(2,1) G_{k\uparrow d\uparrow}^{>}(1,2) - T_{2,k} T_{3,k'}^* G_{k'\uparrow k\uparrow}^{<}(2,1) G_{d\uparrow d\uparrow}^{>}(1,2) - T_{2,k}^* T_{3,k'} G_{d\uparrow d\uparrow}^{<}(2,1) G_{k\uparrow k'\uparrow}^{>}(1,2)] \quad (2)$$

where we have used abbreviation $G(t_1, t_2) = G(1, 2)$ and we have used k and k' to label, respectively, the second and third superconducting lead. The Green's functions $\mathbf{G}^{r,a,<,>}$ in 2×2 Nambu representation take the following forms¹⁴⁻¹⁶

$$G_{\alpha\beta}^{r,a}(t_1, t_2) = \mp i \theta(\pm t_1 \mp t_2) \times \begin{pmatrix} \langle \{X_{\alpha\uparrow}(t_1), Y_{\beta\uparrow}^+(t_2)\} \rangle & \langle \{X_{\alpha\uparrow}(t_1), Y_{\beta\downarrow}(t_2)\} \rangle \\ \langle \{X_{\alpha\downarrow}^+(t_1), Y_{\beta\uparrow}^+(t_2)\} \rangle & \langle \{X_{\alpha\downarrow}^+(t_1), Y_{\beta\downarrow}(t_2)\} \rangle \end{pmatrix}$$

$$G_{\alpha\beta}^{<}(t_1, t_2) = i \begin{pmatrix} \langle Y_{\beta\uparrow}^+(t_2) X_{\alpha\uparrow}(t_1) \rangle & \langle Y_{\beta\downarrow}(t_2) X_{\alpha\uparrow}(t_1) \rangle \\ \langle Y_{\beta\uparrow}^+(t_2) X_{\alpha\downarrow}^+(t_1) \rangle & \langle Y_{\beta\downarrow}(t_2) X_{\alpha\downarrow}^+(t_1) \rangle \end{pmatrix}$$

$$G_{\alpha\beta}^{>}(t_1, t_2) = -i \begin{pmatrix} \langle X_{\alpha\uparrow}(t_1) Y_{\beta\uparrow}^+(t_2) \rangle & \langle X_{\alpha\uparrow}(t_1) Y_{\beta\downarrow}(t_2) \rangle \\ \langle X_{\alpha\downarrow}^+(t_1) Y_{\beta\uparrow}^+(t_2) \rangle & \langle X_{\alpha\downarrow}^+(t_1) Y_{\beta\downarrow}(t_2) \rangle \end{pmatrix}$$

where X and Y stand for the annihilation operators, such as $C_{1,p}$, $C_{n,k}$, and d . These Green's functions satisfy the general relation, $\mathbf{G}^{>} = \mathbf{G}^{<} + \mathbf{G}^r - \mathbf{G}^a$. Using the Keldysh equation¹⁷

$$\mathbf{G}^{<,>} = (1 + \mathbf{G}^r \Sigma^r) \mathbf{G}_0^{<,>} (1 + \Sigma^a \mathbf{G}^a) + \mathbf{G}^r \Sigma^{<} \mathbf{G}^a$$

we have the following relations

$$G_{d\uparrow k\uparrow}^{<,>}(t_1, t_2) = T_{2,k}^* \int dt [G_{d\uparrow d\uparrow}^r(t_1, t) g_{k\uparrow k\uparrow}^{<,>}(t, t_2) + G_{d\uparrow d\uparrow}^{<,>}(t_1, t) g_{k\uparrow k\uparrow}^a(t, t_2) + G_{d\uparrow d\downarrow}^r(t_1, t) g_{k\downarrow k\uparrow}^{<,>}(t, t_2) + G_{d\uparrow d\downarrow}^{<,>}(t_1, t) g_{k\downarrow k\uparrow}^a(t, t_2)] \quad (3)$$

$$G_{k\uparrow d\uparrow}^{<,>}(t_1, t_2) = T_{2,k} \int dt [g_{k\uparrow k\uparrow}^{<,>}(t_1, t) G_{d\uparrow d\uparrow}^a(t, t_2) + g_{k\uparrow k\uparrow}^r(t_1, t) G_{d\uparrow d\uparrow}^{<,>}(t, t_2) + g_{k\uparrow k\downarrow}^{<,>}(t_1, t) G_{d\downarrow d\uparrow}^a(t, t_2) + g_{k\uparrow k\downarrow}^r(t_1, t) G_{d\downarrow d\uparrow}^{<,>}(t, t_2)] \quad (4)$$

$$\begin{aligned}
G_{k\uparrow k'\uparrow}^{<, >}(t_1, t_2) &= T_{3, k'}^* \int dt [G_{k\uparrow d\uparrow}^r(t_1, t) g_{k'\uparrow k'\uparrow}^{<, >}(t, t_2) \\
&+ G_{k\uparrow d\uparrow}^{<, >}(t_1, t) g_{k'\uparrow k'\uparrow}^a(t, t_2) + G_{k\uparrow d\downarrow}^r(t_1, t) g_{k'\downarrow k'\uparrow}^{<, >}(t, t_2) \\
&+ G_{k\uparrow d\downarrow}^{<, >}(t_1, t) g_{k'\downarrow k'\uparrow}^a(t, t_2)] \quad (5)
\end{aligned}$$

where $G_{k\uparrow, d\sigma}^r$ is given by

$$\begin{aligned}
G_{k\uparrow d\sigma}^r(t_1, t_2) &= T_{2, k} \int dt [g_{k\uparrow k\uparrow}^r(t_1, t) G_{d\uparrow d\sigma}^r(t, t_2) \\
&+ g_{k\uparrow k\downarrow}^r(t_1, t) G_{d\downarrow d\sigma}^r(t, t_2)] \quad (6)
\end{aligned}$$

Substituting the above relations to Eq.(1) and taking the Fourier transform, we obtain

$$\begin{aligned}
P_{23} &= -4e^2 \Gamma_2 \Gamma_3 \int \frac{dE}{2\pi} \{ (\mathbf{G}^r \mathbf{g}^< + \mathbf{G}^< \mathbf{g}^a)_{\uparrow\uparrow} (\mathbf{G}^r \mathbf{g}^> \\
&+ \mathbf{G}^> \mathbf{g}^a)_{\uparrow\uparrow} + (\mathbf{g}^< \mathbf{G}^a + \mathbf{g}^r \mathbf{G}^<)_{\uparrow\uparrow} (\mathbf{g}^> \mathbf{G}^a + \mathbf{g}^r \mathbf{G}^>)_{\uparrow\uparrow} \\
&- G_{\uparrow\uparrow}^> \{ (\mathbf{g}^r \mathbf{G}^r \mathbf{g}^<)_{\uparrow\uparrow} + [(\mathbf{g}^< \mathbf{G}^a + \mathbf{g}^r \mathbf{G}^<) \mathbf{g}^a]_{\uparrow\uparrow} \} \\
&- G_{\uparrow\uparrow}^< \{ (\mathbf{g}^r \mathbf{G}^r \mathbf{g}^>)_{\uparrow\uparrow} + [(\mathbf{g}^> \mathbf{G}^a + \mathbf{g}^r \mathbf{G}^>) \mathbf{g}^a]_{\uparrow\uparrow} \} \} \quad (7)
\end{aligned}$$

where $\Gamma_\alpha = 2\pi \sum_k \rho_{N\alpha} |T_{\alpha k}|^2$ with $\alpha = 2, 3$ are the linewidth functions. Here $\rho_{N2,3}$ are the normal density of states of the superconducting leads 2 and 3. We have used the wide-band limit¹⁸ and thus the linewidth function is independent of the energy. $G_{\sigma\sigma'}^{r,a,<,>} \equiv G_{d\sigma d\sigma'}^{r,a,<,>}$ are the full Green's functions for the quantum dot in presence of the leads, while $g_{\sigma\sigma'}^{r,a,<,>}$ are the exact Green's functions for BCS superconductor in the absence of the coupling between the leads and quantum dot. Eq.(7) is the central result of this paper. It describes the cross correlation for a three-terminal hybrid N-S-S system and is valid at any temperature and finite voltage, i.e., valid for both $eV \geq \Delta$ and $eV < \Delta$. In order to calculate this correlation, one must know all the Green's functions. The exact Green's functions $g_{\sigma\sigma'}^{r,a,<}$ for the isolated superconducting leads are^{19,20}

$$\mathbf{g}^r(E) = -\frac{i\zeta(E)}{2\sqrt{E^2 - \Delta^2}} \begin{pmatrix} E & \Delta \\ \Delta & E \end{pmatrix} = [\mathbf{g}^a(E)]^+$$

$$\mathbf{g}^<(E) = if(E)\theta(|E| - \Delta) \frac{\zeta(E)}{\sqrt{E^2 - \Delta^2}} \begin{pmatrix} E & \Delta \\ \Delta & E \end{pmatrix}$$

where $f(E) = 1/[\exp(\beta(E - E_F)) + 1]$ is the well known Fermi distribution function, $\theta(x)$ is the step function and $\zeta(E) = 1$ when $E > -\Delta$, otherwise $\zeta(E) = -1$. We will choose the Fermi energy of the normal lead in line with the chemical potential μ_s of superconducting condensate which is set to zero, i.e., $E_F = \mu_s = 0$. The retarded Green's function for the quantum dot can be calculated using the Dyson equation

$$\mathbf{G}^r(E) = \frac{1}{[\mathbf{G}_0^r(E)]^{-1} - \mathbf{\Sigma}^r(E)}$$

with

$$\mathbf{G}_0^r(E) = \frac{1}{\begin{pmatrix} E - \epsilon_0 & 0 \\ 0 & E + \epsilon_0 \end{pmatrix}}$$

and

$$\mathbf{\Sigma}^r(E) = -\frac{i}{2}\Gamma_1 \begin{pmatrix} 1 & 0 \\ 0 & 1 \end{pmatrix} - \frac{i}{2}(\Gamma_2 + \Gamma_3) \frac{\zeta(E)}{\sqrt{E^2 - \Delta^2}} \begin{pmatrix} E & \Delta \\ \Delta & E \end{pmatrix}$$

The lesser Green's function can be obtained from the Keldysh equation $\mathbf{G}^< = \mathbf{G}^r \mathbf{\Sigma}^< \mathbf{G}^a$. Here the lesser self-energy is given by

$$\begin{aligned}
\mathbf{\Sigma}^<(E) &= i\Gamma_1 \begin{pmatrix} f(E + eV) & 0 \\ 0 & f(E - eV) \end{pmatrix} + \\
&if(E)\theta(|E| - \Delta) \frac{\Gamma_2 + \Gamma_3}{\sqrt{E^2 - \Delta^2}} \zeta(E) \begin{pmatrix} E & \Delta \\ \Delta & E \end{pmatrix}
\end{aligned}$$

Let's first consider the case that external voltage is smaller than the gap energy and consider zero temperature behavior so that there is no quasiparticles participating the transport. In this case, only two-electron current exists, i.e., the current from incoming electron and Andreev reflected hole, we have $\mathbf{g}^r = \mathbf{g}^a$ and $\mathbf{g}^{<,>} = 0$. using the fact that

$$\mathbf{G}^< = i\Gamma_1 \mathbf{G}^r \begin{pmatrix} f_+ & 0 \\ 0 & f_- \end{pmatrix} \mathbf{G}^a \quad (8)$$

and

$$\mathbf{G}^> = i\Gamma_1 \mathbf{G}^r \begin{pmatrix} f_+ - 1 & 0 \\ 0 & f_- - 1 \end{pmatrix} \mathbf{G}^a \quad (9)$$

Eq.(7) can be further simplified as

$$\begin{aligned}
P_{23} &= \frac{e^2 \Gamma_1^2 \Gamma_2 \Gamma_3 \Delta^2}{\Delta^2 - E^2} \int \frac{dE}{2\pi} f_- (1 - f_+) \\
&\times |G_{\uparrow\uparrow}^r G_{\downarrow\downarrow}^a - G_{\uparrow\downarrow}^r G_{\downarrow\uparrow}^a|^2 \\
&= \frac{4e^2 \Gamma_2 \Gamma_3}{(\Gamma_2 + \Gamma_3)^2} \int \frac{dE}{2\pi} f_- (1 - f_+) \\
&\times T_A(E) (1 - T_A(E)) \quad (10)
\end{aligned}$$

where $T_A(E) = \Gamma_1^2 G_{\uparrow\downarrow}^r G_{\downarrow\uparrow}^a$ is the Andreev reflection coefficient and $f_\pm(E) = f(E \pm eV)$. Just as we expected, Eq.(10) is a positive quantity. To get more physical insight, we will assume that eV are small enough and we will keep only the first order in V in Eq.(10). We have

$$\begin{aligned}
P_{23} &= \frac{\Gamma_1^2 \Gamma_2 \Gamma_3 e^3 V}{\pi [\epsilon_0^2 + \frac{\Gamma_1^2}{4} + \frac{(\Gamma_2 + \Gamma_3)^2}{4}]^4} \\
&\times \{ \epsilon_0^4 + \frac{\epsilon_0^2 [\Gamma_1^2 + (\Gamma_2 + \Gamma_3)^2]}{2} + \frac{[\Gamma_1^2 - (\Gamma_2 + \Gamma_3)^2]^2}{4} \} \quad (11)
\end{aligned}$$

For $eV > \Delta$, we have to calculate P_{23} numerically which is presented in the next section.

III. RESULT AND DISCUSSION

We first use Eq.(10) to calculate the cross correlation at finite voltage while keeping $eV < \Delta$. In the following, we will use Δ as the unit of energy and study the symmetric case where $\Gamma_2 = \Gamma_3$. In Fig.1 we show the cross correlation versus the gate voltage at fixed external bias $eV = 0.6$. Four different sets of coupling constants Γ are chosen: (1). $\Gamma_1 = 0.8$ and $\Gamma_2 = 0.8$. In this case, it represents the strong coupling between leads and the quantum dot. The cross correlation (solid line) displays two broad peaks located symmetrically at $ev_g = \pm 0.6$. (2). $\Gamma_1 = 0.8$ and $\Gamma_2 = 0.1$. In this case, the normal lead couples strongly with the quantum dot while the superconducting leads couple weakly. The cross correlation (dotted line) exhibits a single peak at $v_g = 0$. (3). $\Gamma_1 = 0.1$ and $\Gamma_2 = 0.8$. This is the reverse of case (2). We see that the cross correlation (dot-dashed line) shows a flat region near $v_g = 0$. (4). $\Gamma_1 = 0.1$ and $\Gamma_2 = 0.1$. This is the weak coupling case. The cross correlation (dashed line) has two sharp peaks close to $v_g = 0$ and decays quickly away from it. To understand these features, we notice that two terms ($F_1 = \int dE T_A(E)$ and $F_2 = \int dE T_A^2(E)$) in Eq.(10) tend to cancel each other. In the strong coupling case, the contribution from both terms are of the same order of magnitude. Both show broad peak near $v_g = 0$ with the second term decreasing faster away from $v_g = 0$ (see Fig.2a). As a result, we obtain the double-peak structure as shown in Fig.1. When $\Gamma_1 = 0.8$ and $\Gamma_2 = 0.1$, the contribution from F_2 is much smaller than that of F_1 and hence just one peak shows up (Fig.2b). For $\Gamma_1 = 0.1$ and $\Gamma_2 = 0.8$, the addition of F_1 and F_2 gives a long plateau between $ev_g = -0.5$ and $ev_g = 0.5$ (Fig.2c). In the weak coupling regime, F_1 and F_2 give comparable contributions with a single peak. Similar to the strong coupling case, the integral of F_2 decreases faster than that of F_1 resulting again a double-peak structure (Fig.2d). As one decreases the external bias to $eV = 0.2$, the cross correlation in the strong coupling case still shows double peak structure with smaller amplitude (Fig.3). We also find that the peak position is shifted towards origin and peak to valley ratio becomes much smaller. In the weak coupling regime, the cross correlation is roughly unchanged. In the case of $\Gamma_1 = 0.8$ and $\Gamma_2 = 0.1$ (or vice versa), the cross correlation decreases. Now we examine the cross correlation versus external bias at fixed energy levels. Fig.4a displays the cross correlation P_{23} versus external voltage when $\epsilon_0 = 0$. We see that, except for $\Gamma_1 = 0.8$ and $\Gamma_2 = 0.1$ that P_{23} increases monotonically, P_{23} develops a plateau region for the other three sets of coupling parameters. These plateau regions are due to the resonant tunneling which can be seen from Fig.4b where the differential cross correlation dP_{23}/dV versus external voltage is depicted. Here we see typical behavior of the shot noise²¹: a minimum separated by two peaks. The minimum is due to the resonant Andreev reflection since $dP_{23}/dV \sim T_A(1 - T_A)$. As

one increases the energy level ($\epsilon_0 = 0.3$), the dip between two peaks can no longer reach zero indicating that the maximum Andreev reflection coefficient T_A is much less than one. We also note that for $\Gamma_1 = 0.1$ and $\Gamma_2 = 0.8$, only one peak is left and resonant feature disappeared.

To study the effect of quasiparticle when $eV > \Delta$, we calculate the cross correlation using Eq.(7). Fig.6 shows the cross correlation versus external voltage at $\epsilon_0 = 0.0$. We see that once the voltage is larger than the gap energy Δ , the cross correlation decreases quickly indicating Fermionic contributions. For the strong coupling case, P_{23} becomes negative in the large V limit. This can be understood as follows. When $eV > \Delta$, electrons with energy less than eV will all participate in transport. In particular, for incoming electrons with energy inside the superconducting gap, only two-electron current is allowed and hence the contribution to the cross correlation should be positive as we just discussed above. However, when the energy of incoming electron is outside of the gap the current comes from four processes^{22,14}: (1). Andreev reflection; (2). the conventional electron tunneling through the system; (3). "Branch crossing" process²²: an electron incident from the normal lead converting into a hole like in the superconducting leads; (4). An electron (or a hole) incident from the normal lead tunnels into the superconducting lead, picks up a quasiparticle (or a quasihole) in the superconducting lead and creates (or annihilates) a Cooper pair. In these processes, the latter three give negative contributions to the cross correlation. Competition between Andreev reflection process and the rest of three processes give rise either positive or negative cross correlation depending on which process dominates (see Fig.6). Typically, near the resonance the Breit-Wigner form for the Andreev reflection coefficient reads^{23,24}

$$T_A = \frac{\Gamma_1^2 \Gamma_2^2}{4(E^2 - \epsilon_0^2 + \Gamma \delta \Gamma / 4)^2 + \Gamma_1^2 \Gamma_2^2 + \epsilon_0^2 (\Gamma + \delta \Gamma)^2} \quad (12)$$

and transmission coefficient for normal tunneling process

$$T = \frac{\Gamma_1 \Gamma_2}{(E - \epsilon_0)^2 + \Gamma^2 / 4} \quad (13)$$

where $\Gamma = \Gamma_1 + \Gamma_2$ and $\delta \Gamma = \Gamma_1 - \Gamma_2$. We see that the Andreev reflection is suppressed when off resonance. Furthermore, at large external bias if the resonant energy is outside of the gap, the Andreev reflection is drastically suppressed and normal tunneling is allowed at certain energy. Therefore, we expect negative cross correlation in this case. In Fig.7, we depict P_{23} versus V at $\epsilon_0 = 2.0$. Since the resonant level is outside of the gap, the plateau region for P_{23} when eV is inside the gap disappeared. We see that except for the case of $\Gamma_1 = 0.8$ and $\Gamma_2 = 0.1$, P_{23} becomes negative at large voltages. Our numerical result shows that at even larger ϵ_0 , the transport of quasiparticle dominates and all P_{23} are negative at large external voltage. Finally, we plot in Fig.8 the P_{23} versus v_g at

$eV = 4$. We see that at large voltages, all the cross correlation functions become negative. For the strong coupling case, we observe oscillations of P_{23} between Bosonic and Fermionic behaviors due to the competition between entangled electron pair and the quasiparticles. This can be easily checked experimentally by changing the gate voltage.

In summary, we have proposed an entangled electron pair HBT experiment by using the three-terminal N-S-S hybrid mesoscopic system. When the external voltage is less than the gap energy, only two-electron current is present. The cross correlation is found to be positive, which demonstrates that this entangled electron pair looks like the composite Boson and tends to bunch in cluster. However, when the external voltage is larger than the gap energy the quasiparticle will participate the transport which gives the Fermionic contribution to the cross correlation. As the result of competition between Andreev reflection process and the other tunneling process involving quasiparticles, the cross correlation can be either positive or negative depending on which one dominates. For the strong coupling case and at large external voltage, the cross correlation function changes sign as one varies the gate voltage which controls the position of the resonant level.

ACKNOWLEDGMENTS

We gratefully acknowledge support by a RGC grant from the SAR Government of Hong Kong under grant number HKU 7091/01P and a CRCG grant from the University of Hong Kong.

a) Electronic mail: jianwang@hkusub.hku.hk

-
- ¹ E. Fermi, Zeits. f. Phys. **36**, 902 (1926); P.A.M. Dirac, Proc. Roy. Soc. London A **112**, 661 (1926).
 - ² S.N. Bose, Zeits. f. Phys. **26**, 178 (1924).
 - ³ L.D. Landau and E.M. Lifshitz, Statistical physics, (Pergamon Press, Oxford, (1980)).
 - ⁴ Ya.M. Blanter and M. Buttiker, Phys. Rep. **336**, 2 (2000).
 - ⁵ R. Hanbury Brown and R.Q. Twiss, Nature (London), **177**, 27 (1956).
 - ⁶ M. Henny et al., Science, **284**, 296 (1999).
 - ⁷ W.D. Oliver et al., Science, **284**, 299 (1999).
 - ⁸ G. Burkard, D. Loss, and E.V. Sukhorukov, Phys. Rev. B **61**, R16303 (2000).
 - ⁹ J. Torriès and Th. Martin, Eur. Phys. J. B **12**, 319 (1999).
 - ¹⁰ P. Samueisson and M. Buttiker, cond-mat/0203188.
 - ¹¹ J. Borlin, W. Belzig, and C. Bruder, Phys. Rev. Lett. **88**, 197001 (2002).
 - ¹² G.B. Lesovik, T. Martin, and G. Blatter, Eur. Phys. J. B **24**, 287 (2001).

- ¹³ K.E. Nagaev, Phys. Rev. B **64**, R81304 (2001).
- ¹⁴ J.C. Cuevas, A. Martin-Rodero, and A. Levy Yeyati, Phys. Rev. B **54**, 7366 (1996).
- ¹⁵ Q.F. Sun, J. Wang, T.H. Lin, Phys. Rev. B **59**, 3831 (1999).
- ¹⁶ Q.F. Sun, B.G. Wang, J. Wang, T.H. Lin, Phys. Rev. B **61**, 4754 (2000).
- ¹⁷ J. Rammer and H. Smith, Rev. Mod. Phys. **58**, 323 (1986).
- ¹⁸ A.P. Jauho et. al., Phys. Rev. B **50**, 5528 (1994).
- ¹⁹ J. Wang, Y.D. Wei, H. Guo, Q.F. Sun, T.H. Lin, Phys. Rev. B **64**, 104508 (2001).
- ²⁰ Here the density of state in the Green's function has been absorbed in the linewidth function Γ .
- ²¹ Y.D. Wei, B.G. Wang, J. Wang, and H. Guo, Phys. Rev. B **60**, 16900 (1999).
- ²² G.E. Blonder, M. Tinkham, T.M. Klapwijk, Phys. Rev. B **25**, 4515 (1982).
- ²³ C.W.J. Beenakker, Rev. Mod. Phys. **69**, 731 (1997).
- ²⁴ Y.D. Wei, J. Wang, H. Guo, H. Mehrez, and C. Roland, Phys. Rev. B **63**, 195412 (2001).

FIG. 1. The cross correlation P_{23} versus gate voltage at $eV = 0.6$ for different coupling parameters: (1). $\Gamma_1 = 0.8$ and $\Gamma_2 = 0.8$ (solid line); (2). $\Gamma_1 = 0.8$ and $\Gamma_2 = 0.1$ (dotted line); (3). $\Gamma_1 = 0.1$ and $\Gamma_2 = 0.8$ (dot-dashed line); (4). $\Gamma_1 = 0.1$ and $\Gamma_2 = 0.1$ (dashed line).

FIG. 2. The contribution of F_1 (dotted line) and F_2 (dot-dashed line) to the cross correlation P_{23} (solid line) versus gate voltage at $eV = 0.6$. (a). $\Gamma_1 = 0.8$ and $\Gamma_2 = 0.8$; (b). $\Gamma_1 = 0.8$ and $\Gamma_2 = 0.1$; (c). $\Gamma_1 = 0.1$ and $\Gamma_2 = 0.8$; (d). $\Gamma_1 = 0.1$ and $\Gamma_2 = 0.1$.

FIG. 3. The cross correlation P_{23} versus gate voltage at $eV = 0.2$. The coupling parameters and corresponding symbols are the same as Fig.1.

FIG. 4. (a). The cross correlation versus external voltage at $\epsilon_0 = 0.0$. (b). The differential cross correlation versus external voltage at $\epsilon_0 = 0.0$. The coupling parameters and corresponding symbols are the same as Fig.1.

FIG. 5. The differential cross correlation versus external voltage at $\epsilon_0 = 0.3$. The coupling parameters and corresponding symbols are the same as Fig.1.

FIG. 6. The cross correlation versus external voltage at $\epsilon_0 = 0.0$. The coupling parameters and corresponding symbols are the same as Fig.1.

FIG. 7. The cross correlation versus external voltage at $\epsilon_0 = 2.0$. The coupling parameters and corresponding symbols are the same as Fig.1. For illustration purpose, we have multiplied the cross correlation by a factor of 10 for the dotted line, 5 for the dot-dashed line, and 50 for the dashed line.

FIG. 8. The cross correlation versus gate voltage at $eV = 4.0$. The coupling parameters and corresponding symbols are the same as Fig.1.

Fig1

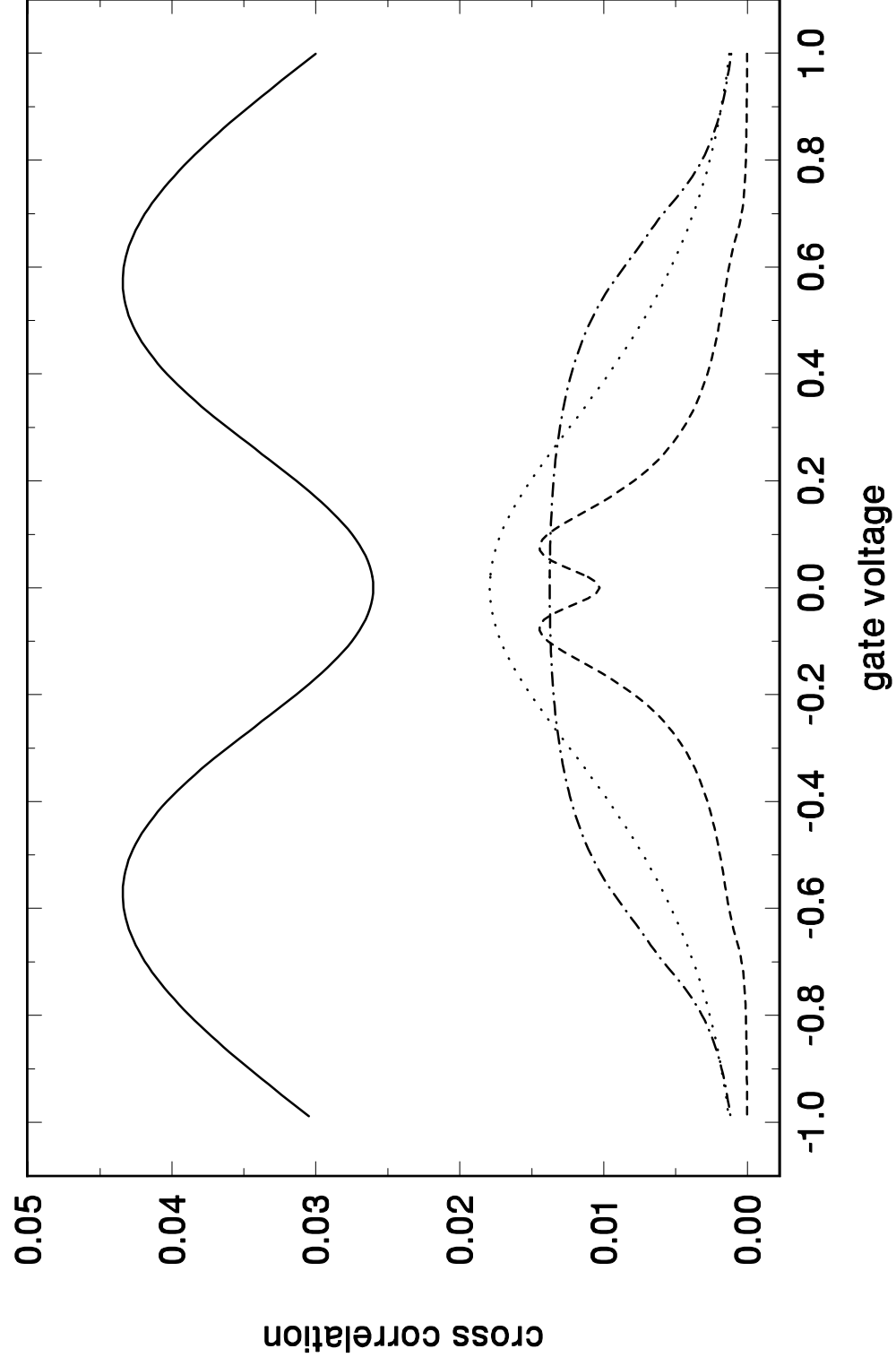


Fig2

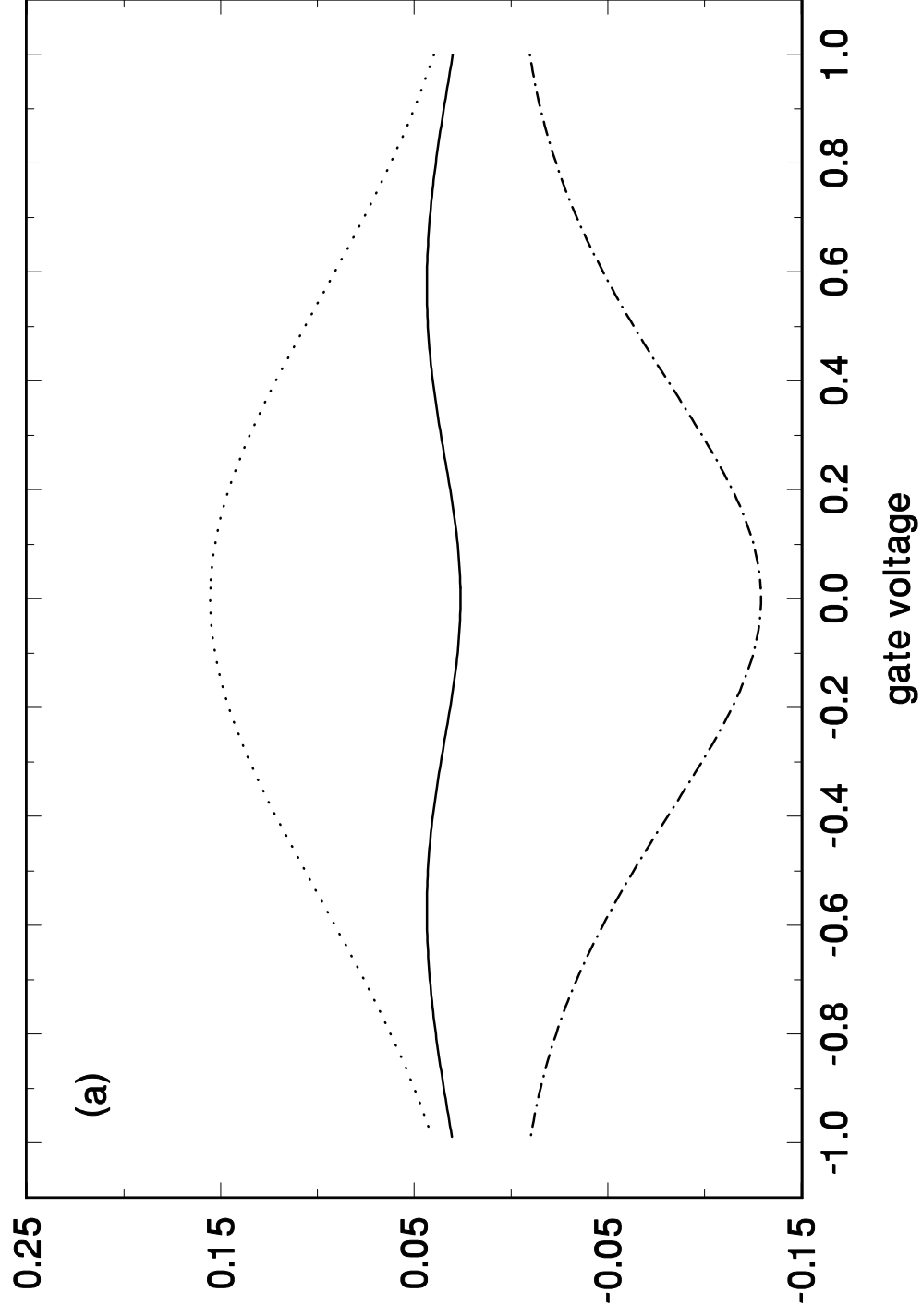


Fig2

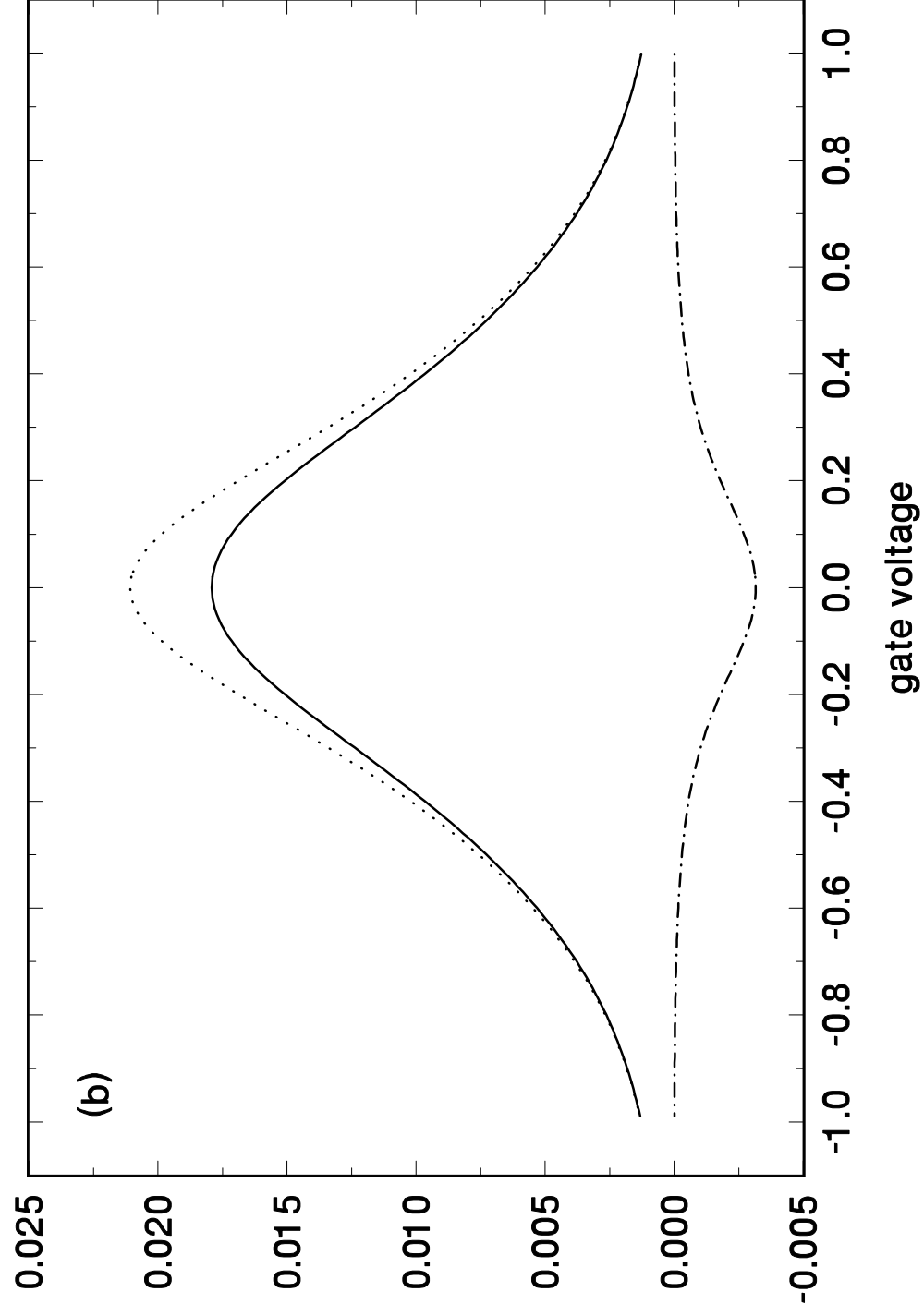


Fig2

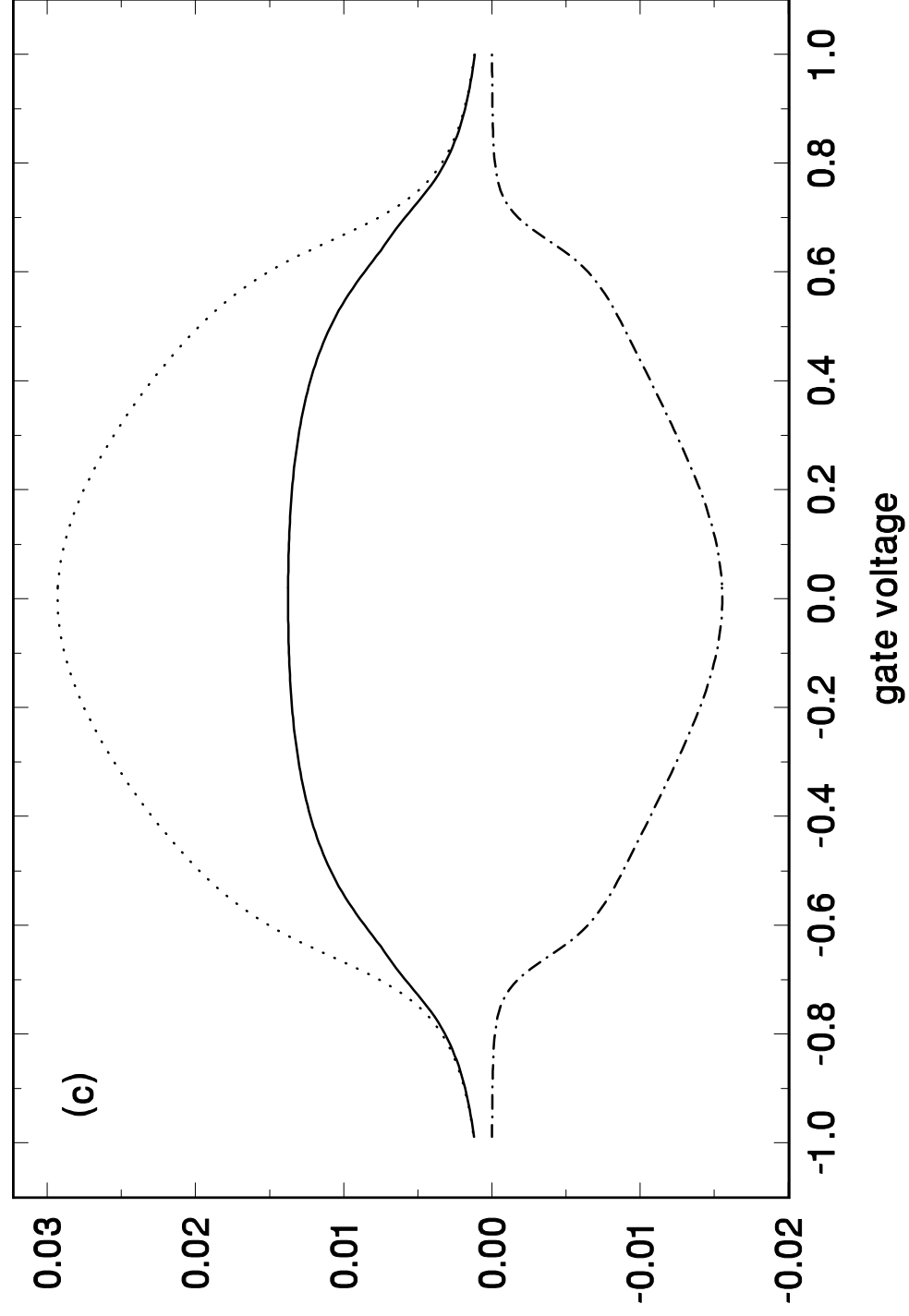


Fig2

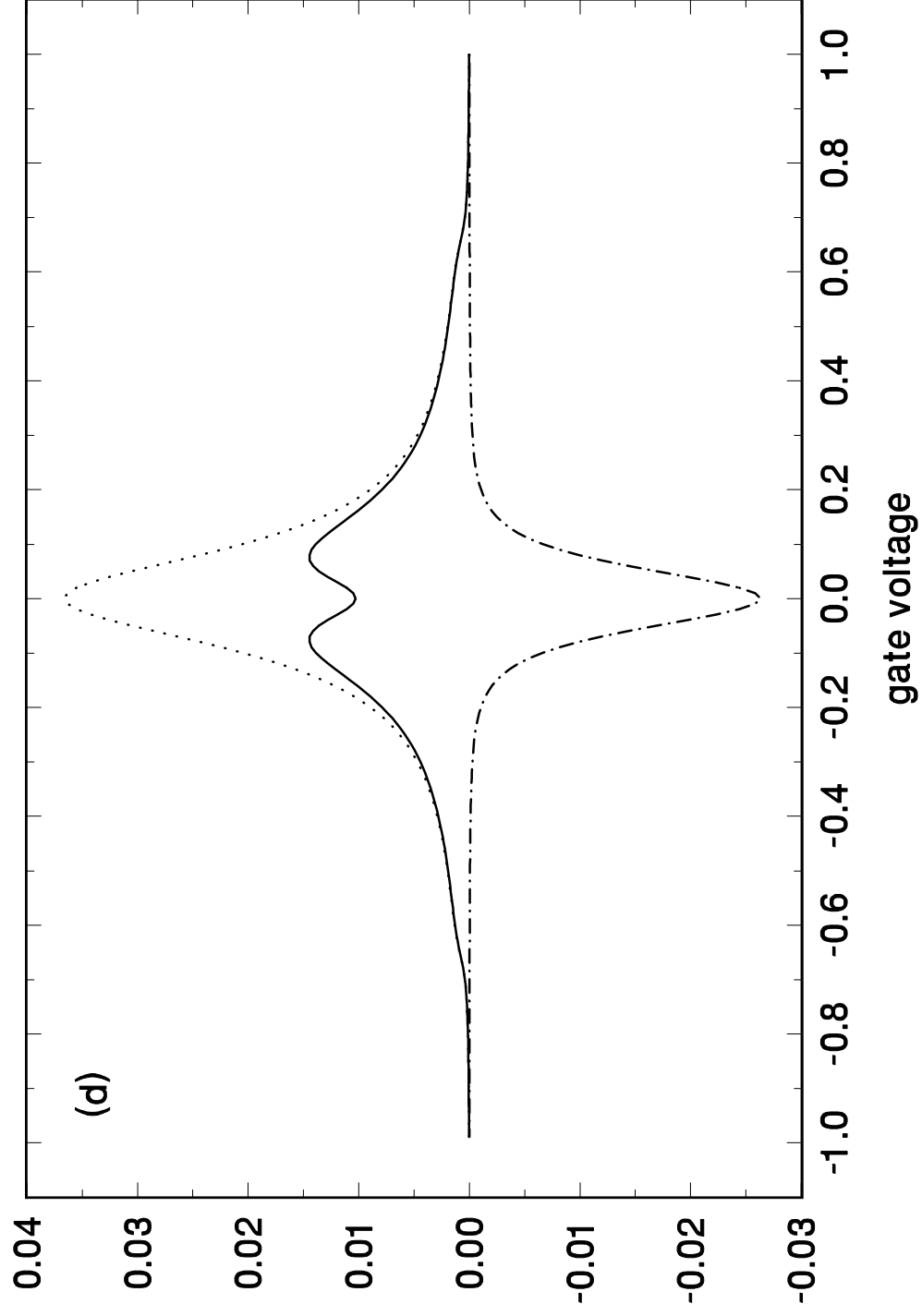


Fig3

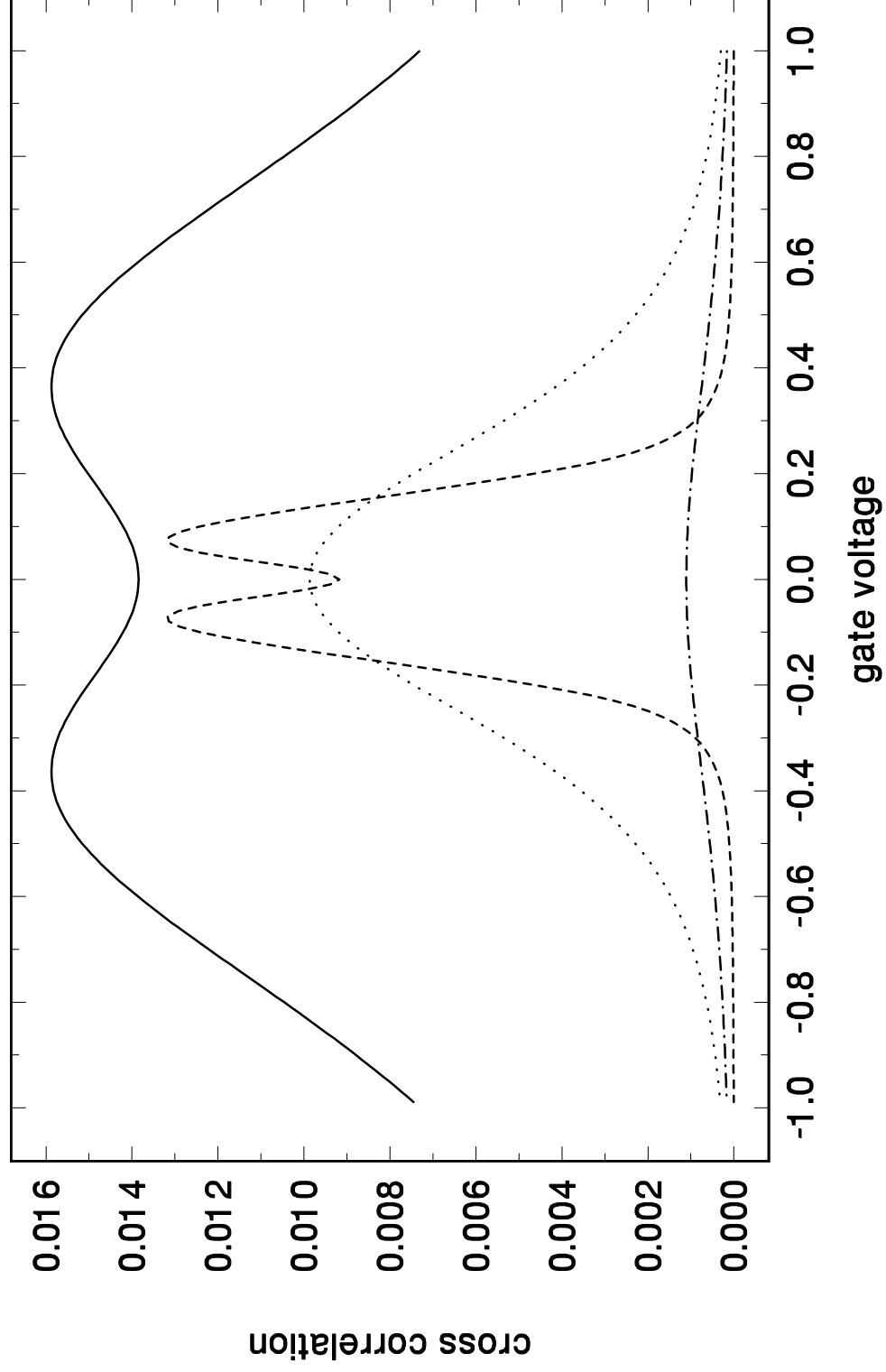


Fig4

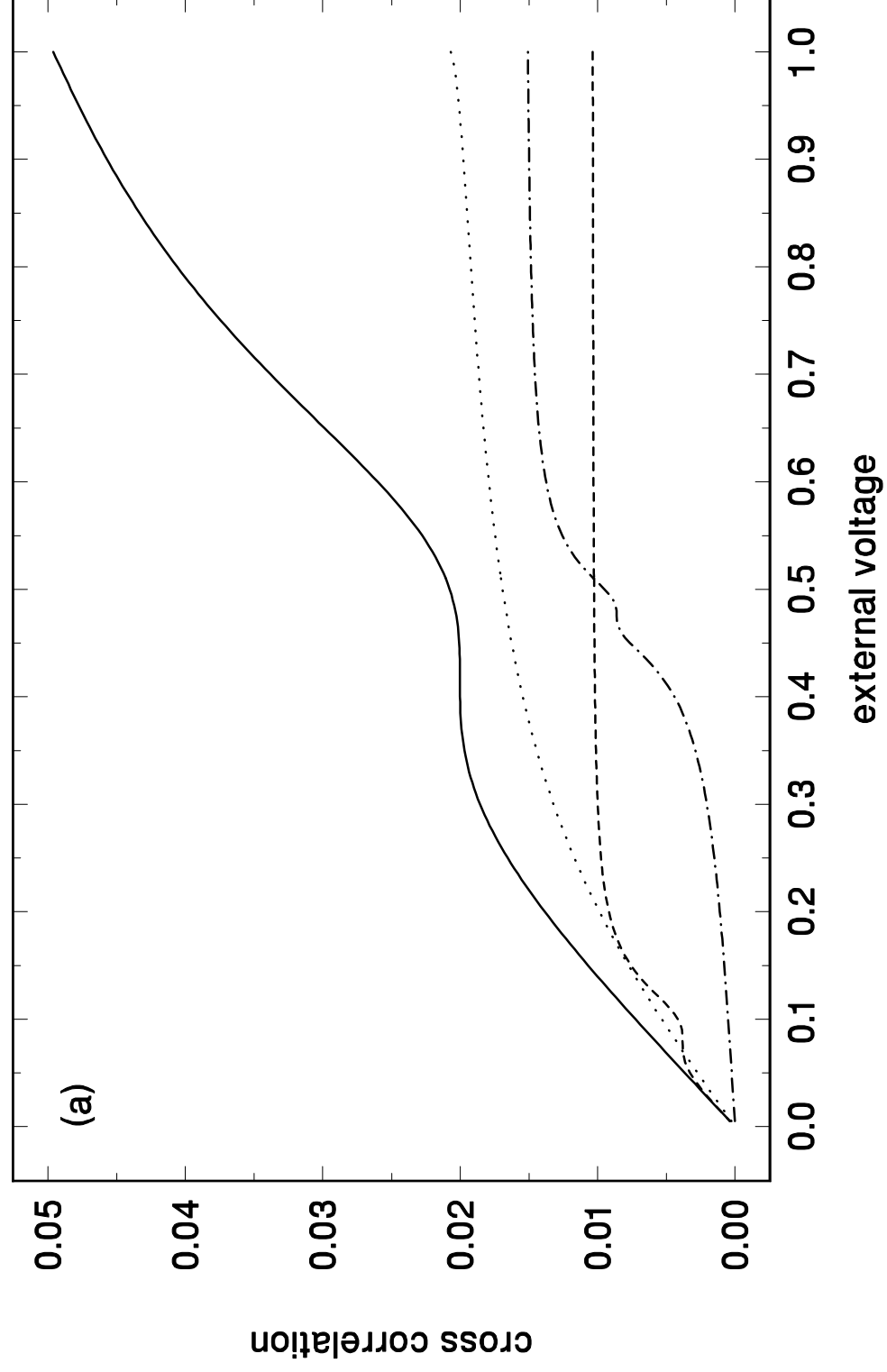


Fig4

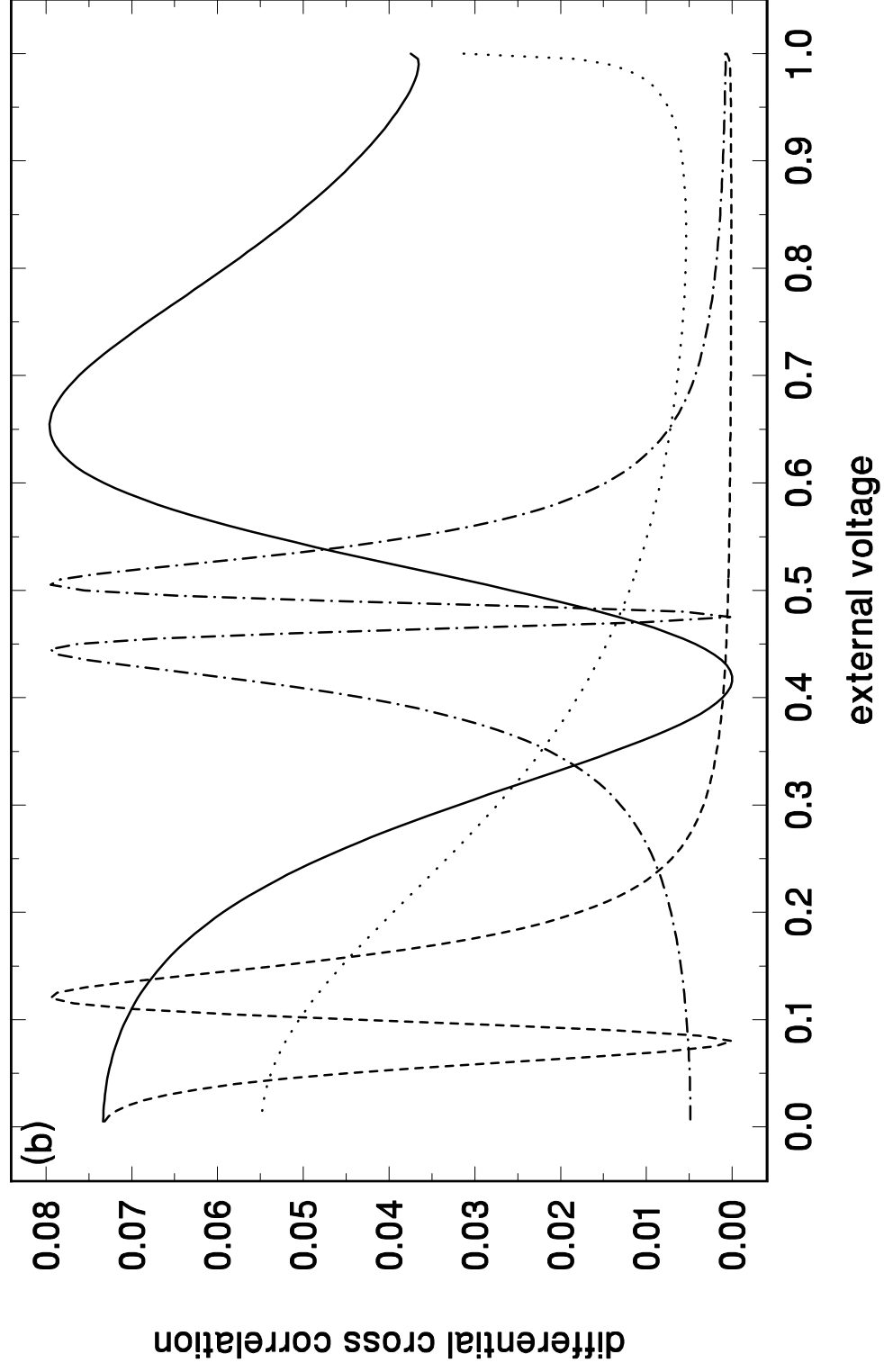


Fig5

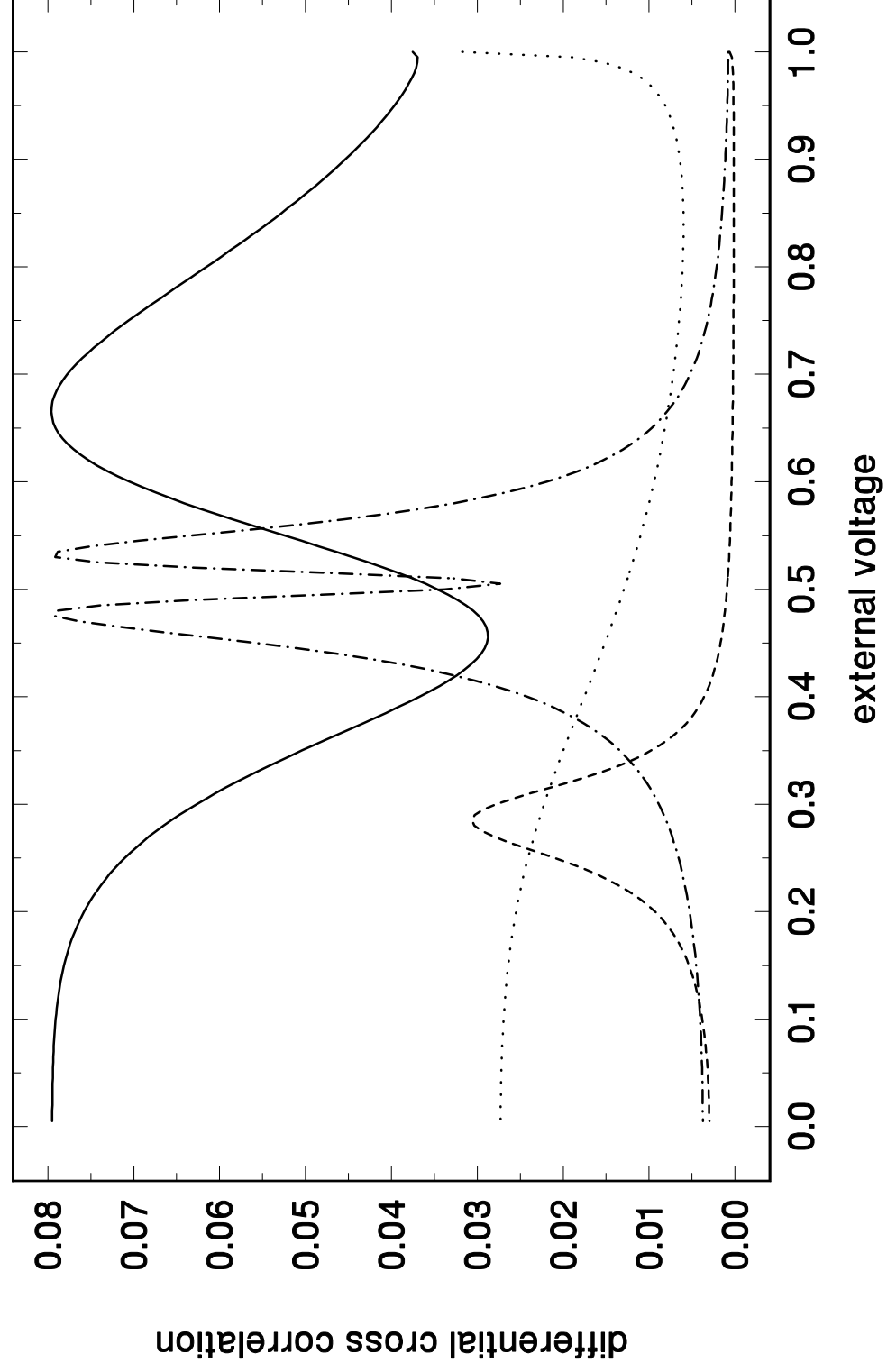


Fig6

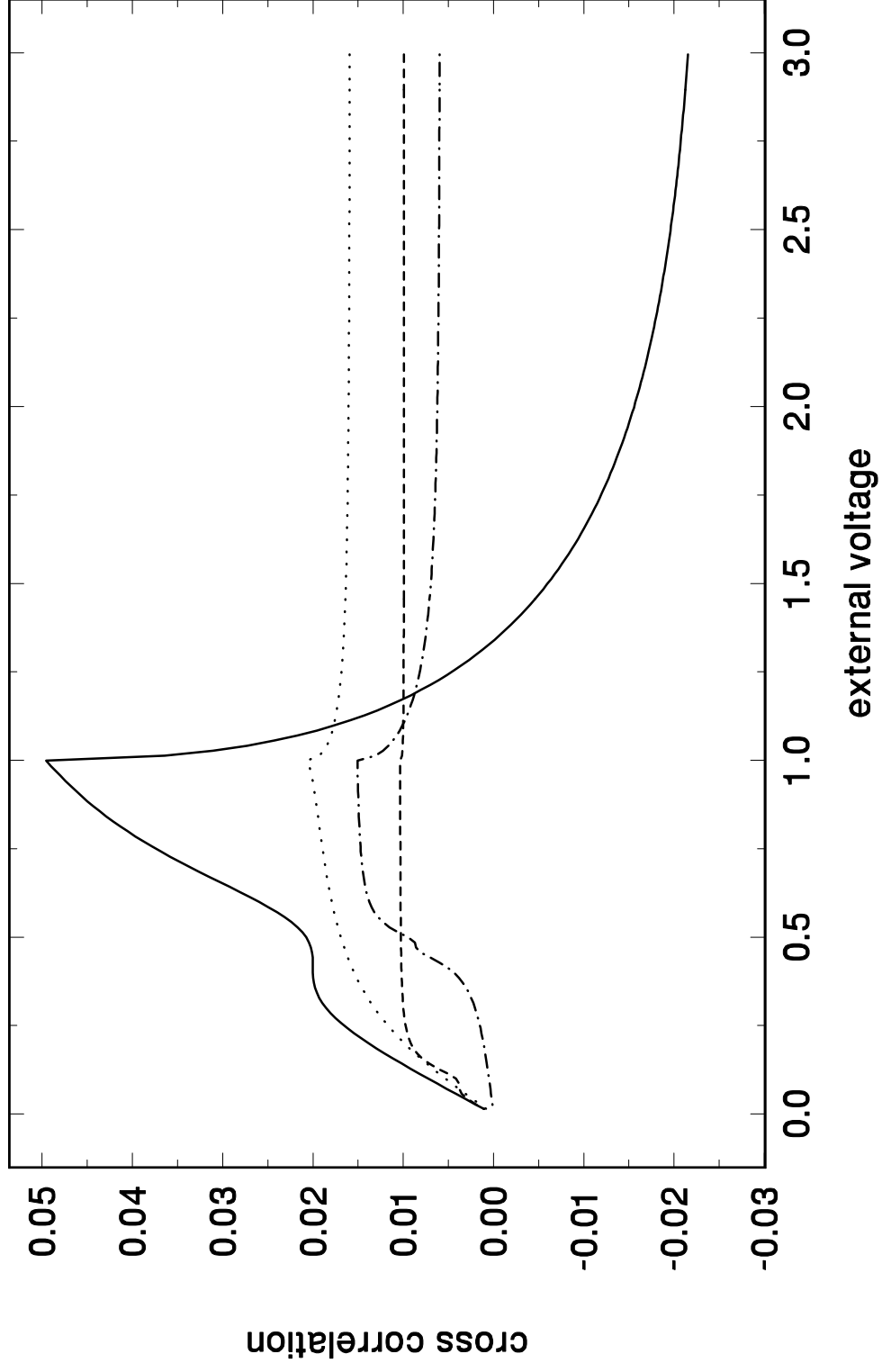


Fig7

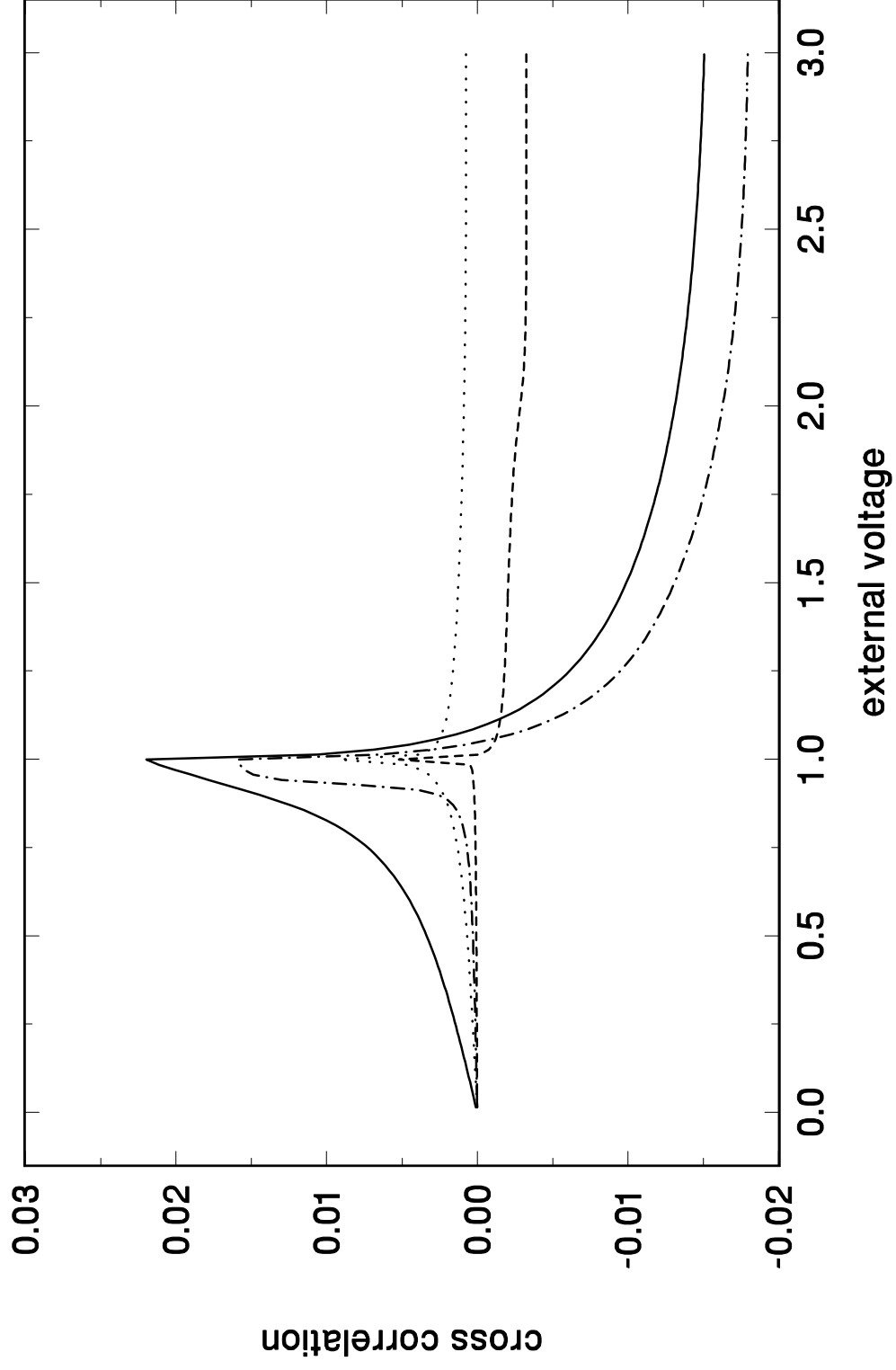


Fig8

